Electronic Supplementary Material (ESI) for Chemical Communications

Supporting Information

Is the Special Pair Structure a Good Strategy for the Kinetics During the Last Step of the Energy Transfer With the Nearest Antenna? A Chemical Model Approach.

Jean-Michel Camus, Adam Langlois, Shawkat Aly, Roger Guilard,* and Pierre D. Harvey*

Table of Content

1. Experimental Section

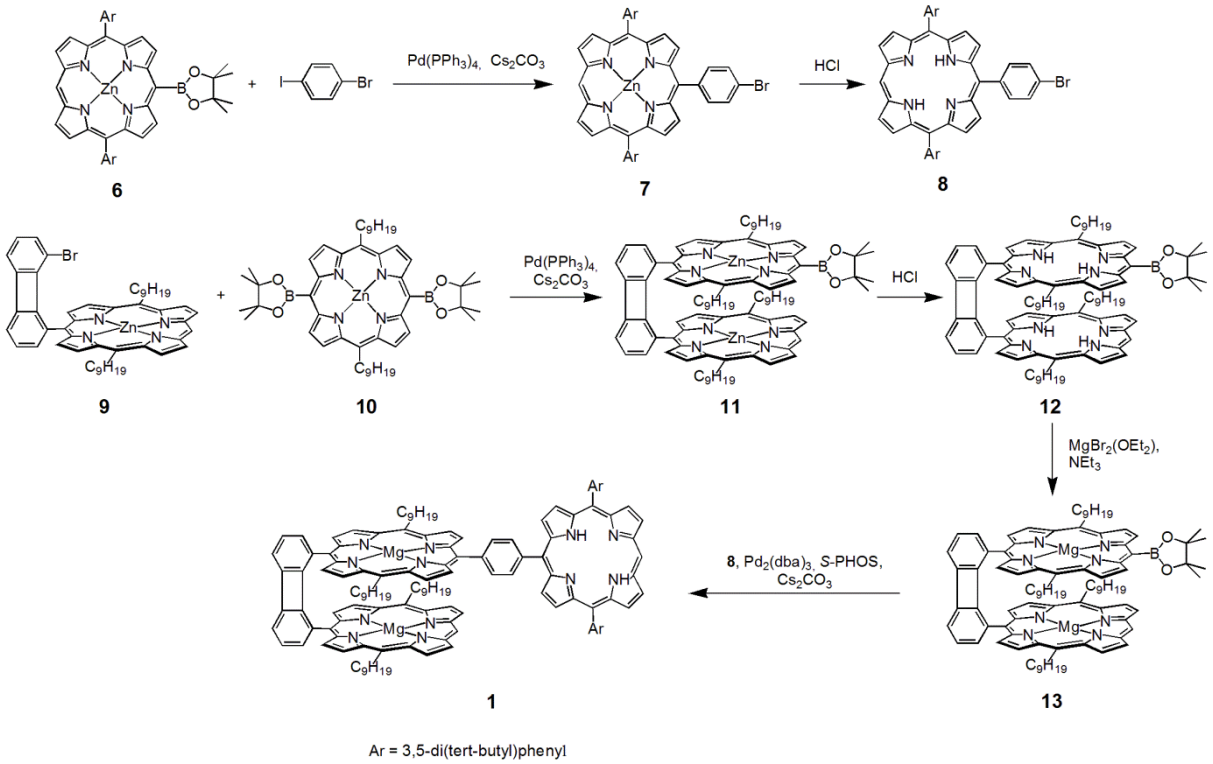

Materials. Zinc(II) 5-(8-bromobiphenylene-1-yl)-10,20-bis(nonyl)porphyrin **9**,[1] zinc(II) 5,15-bis-(4,4,5,5-tetramethyl-1,3,2-dioxaborolan-2-yl)-10,20-bis(nonyl)porphyrin **10,**[1] zinc (II) 5-{8-[zinc(II)-10,20-dinonylporphyrin-5-yl]-biphenylene-1-yl}-15-(4,4,5,5-tetramethyl-[1,3,2]-dioxaborolan-2-yl)-10,20-dinonyl-porphyrin **11**,[1] and zinc (II) 5-(4,4,5,5-tetramethyl-[1,3,2]-dioxaborolan-2-yl)-10,20-bis(3,5-di-*tert*-butylphenyl)porphyrin **6**[2] were synthesized as previously described. The handling of all air/water sensitive materials was carried out using standard high vacuum techniques. Dried toluene was obtained by passing through alumina under nitrogen in the solvent purification systems and then further dried over activated molecular sieves; extra dry DMF was purchased from Aldrich. Triethylamine, dichloromethane and 1,2-dichloroethane were distilled from CaH_2; THF and toluene were distilled from sodium benzophenone ketyl. Unless specified otherwise all other solvents were used as commercially supplied. Silica gel (Merck; 70-120 mm) was used for column chromatography. Analytical thin layer chromatography was performed using Merck 60 F254 silica gel (precoated sheets, 0.2 mm thick). Size exclusion chromatography was carried out under gravity using cross-linked polystyrene Bio-Beads® SX-1 (200 – 400 mesh) in DCM. Reactions were monitored by thin-layer chromatography, UV-vis spectroscopy, and MALDI/TOF mass spectrometry.

Zinc(II) 5-(4-bromophenyl)-10,20-bis-(3,5-di-tert-butyl-phenyl)-porphyrin 7

Under an inert atmosphere, a mixture of zinc (II) 5-(4,4,5,5-tetramethyl-[1,3,2]-dioxaborolan-2-yl)-10,20-bis(3,5-di-*tert*-butyl phenyl)porphyrin (155 mg, 0.18 mmol), 1-bromo,4-iodobenzene (76 mg, 0.27 mmol), cesium carbonate (91 mg, 0.28 mmol), $Pd(PPh_3)_4$ (21 mg, 0.0018 mmol) in 10 mL of anhydrous toluene and 5 mL of DMF was stirred at 100 °C overnight. The reaction was quenched with an aqueous saturated NH_4Cl solution (20 mL). The organic layer was separated, extracted from aqueous phase. The combined organic fractions were washed with water (2 x 20 mL) and dried over $MgSO_4$. The solvent was evaporated and under vacuum and the residue was purified by silica gel (chloroform/petroleum ether 1/4) affording the title compound as a purple solid (0.15 g, 92%). ^{1}H NMR (300.16 MHz, $CDCl_3$): δ 10.30 (s, 1H, *meso*), 9.44 (d, 2H, J = 4.5 Hz, β), 9.18 (d, 2H, J = 4.5 Hz, β), 9.08 (d, 2H, J = 4.7 Hz, β), 8.96 (d, 2H, J = 4.7 Hz, β), 8.15 (d, 4H, J =1.8 Hz, C_6H_3), 8.12 (d, 2H, J = 8.4 Hz, C_6H_4), 7.90 (d, 2H, J = 8.4 Hz, C_6H_4), 7.84 (t, 2H, J =1.8 Hz, C_6H_3) and 1.58 (s, 36H, tBu) ppm. MALDI-TOF MS : *m/z* 902.2 calcd for $C_{54}H_{55}BrN_4Zn$, 902.2 ($M^{+\bullet}$). ESI HRMS : *m/z* 902.2896 calcd for $C_{54}H_{55}BrN_4Zn$, 902.2895 ($M^{+\bullet}$). UV-vis (THF) λmax (log ε)= 414 (5.73), 542 (4.31), 579 (3.30) nm.

5-(4-bromophenyl)-10,20-bis-(3,5-di-tert-butyl-phenyl)-porphyrin 8

20 mL of HCl aqueous solution (4M) was added onto a solution of zinc(II) 5-(4-bromophenyl)-10,20-bis-(3,5-di-tert-butyl-phenyl)porphyrin (0.15 g, 0.166 mmol) in 50 mL of dichloromethane. The reaction mixture was vigourously stirred for 1 hour. The organic layer was separated, washed with a saturated $NaHCO_3$ aqueous solution (2x20 mL) and dried over magnesium sulfate. After evaporation until dryness, the residue was recrystallized in dichloromethane/methanol affording a microcrystalline violet powder (0.14 g, quant.). ^{1}H NMR (300.16 MHz, $CDCl_3$): δ 10.23 (s, 1H, *meso*), 9.35 (d, 2H, J = 4.7 Hz, β), 9.07 (d, 2H, J = 4.6 Hz, β), 8.96 (d, 2H, J = 4.8 Hz, β), 8.84 (d, 2H, J = 4.8 Hz, β), 8.11 (m, 6H, C_6H_4+C_6H_3), 7.87 (d, 2H, J = 8.3 Hz, C_6H_4), 7.83 (m, 2H, C_6H_3), 1.56 (s, 36H, tBu) and -2.94 (s, 2H, NH) ppm. MALDI-TOF MS : *m/z* 840.3 calcd for $C_{54}H_{57}BrN_4$, 840.3 ($M^{+\bullet}$). ESI HRMS : *m/z* 841.3839 calcd for $C_{54}H_{58}BrN_4$, 841.3844 $(M+H)^+$. UV-vis (THF) λmax (log ε)= 412 (5.43), 508 (4.09), 542 (3.69), 584 (3.59), 641 (3.29) nm.

5-{8-[10,20-dinonylporphyrin-5-yl]-biphenylene-1-yl}-15-(4,4,5,5-tetramethyl-[1,3,2]-dioxaborolan-2-yl)-10,20-dinonylporphyrin 12

10 mL of HCl aqueous solution (4M) was added onto a solution of zinc(II) 5-{8-[zinc(II)-10,20-dinonylporphyrin-5-yl]-biphenylene-1-yl}-15-(4,4,5,5-tetramethyl-[1,3,2]-dioxaborolan-2-yl)-10,20-dinonylporphyrin (58 mg, 0.038 mmol) in 15 mL of dichloromethane. The reaction mixture was vigourously stirred for 30 minutes. The acidic layer was removed and 10 mL of HCl aqueous solution (4M) was again added. After stirring for 30 minutes, the organic layer was separated, washed with a saturated $NaHCO_3$ aqueous solution (2x20 mL) and dried over magnesium sulfate. After evaporation until dryness, the residue was purified by silica gel (chloroform/petroleum ether 1/2-2/1) affording the title compound as a purple solid (33 mg, 62%). ^{1}H NMR (300.16 MHz, CD_2Cl_2): δ 9.34 (d, 2H, *J* = 4.6 Hz, β), 9.21 (s, 1H, *meso*), 8.77 (d, 2H, *J* = 4.9 Hz, β), 8.74 (d, 2H, *J* = 5.0 Hz, β), 8.66 (d, 2H, *J* = 4.7 Hz, β), 8.57 (br d, 2H, *J* = 4.9 Hz, β), 8.50 (d, 2H, *J* = 4.9 Hz, β), 8.47 (br d , 2H, *J* = 4.2 Hz, β), 8.37 (d, 2H, *J* = 4.8 Hz, β), 7.35-7.28 (m, 3H, DPB), 7.22-7.12 (m, 3H, DPB), 3.92 (m, 8H, CH_2), 2.13 (s, 12H, CH_3), 1.99 (m, 8H, CH_2), 1.62 (m, 8H, CH_2), 1.45 (m, 8H, CH_2), 1.32 (m, 32H, CH_2), 0.89 (t, 12H, *J* =7.3 Hz, CH_3), -7.13 (s, 2H, NH) and -7.21 (s, 2H, NH) ppm. MALDI-TOF MS: *m/z* 1398.9 calcd for $C_{94}H_{115}BN_8O_2$, 1399.9 ($M+H^+$). ESI HRMS : *m/z* 1399.9323 calcd for $C_{94}H_{116}BN_8O_2$, 1399.9263 ($M+H^+$). UV-vis (THF) λmax (log ε) = 397 (5.54), 517 (4.13), 551 (3.81), 598 (3.68), 652 (3.43) nm.

Magnesium(II) 5-{8-[magnesium(II)-10,20-dinonylporphyrin-5-yl]-biphenylene-1-yl}-15-(4,4,5,5-tetramethyl-[1,3,2]-dioxaborolan-2-yl)-10,20-dinonylporphyrin 13

5-{8-[10,20-dinonylporphyrin-5-yl]-biphenylene-1-yl}-15-(4,4,5,5-tetramethyl-[1,3,2]-dioxaborolan-2-yl)-10,20-dinonylporphyrin (25 mg, 0.018 mmol) was dissolved in 10 mL of dichloromethane and 0.42 mL of NEt_3 (3 mmol) and 0.38 g of $MgBr_2.OEt_2$ (1.5 mmol) were successively added. The reaction mixture was stirred for 30 minutes. 10 mL of dichloromethane was added and the organic phase was washed by a diluted $NaHCO_3$ aqueous solution (2 x 20mL). The organic layer was dried over magnesium sulfate and evaporated until dryness. Chromatographic column on alumina eluting with CH_2Cl_2 and with acetone-CH_2Cl_2 (20%) afforded **3** as purple powder (20 mg, 80%). ^{1}H NMR (300.16 MHz, CD_2Cl_2): δ 9.33 (br s, 2H, β), 9.22(s, 1H, *meso*), 8.74 (m, 4H, β), 8.63 (br s, 2H, β), 8.54 (br s, 2H, β), 8.43 (br s, 2H, β), 8.30 (br s, 2H, β), 8.17 (br s, 2H, β), 7.30-7.23(m, 3H, DPB), 7.16-7.07 (m, 3H, DPB), 3.60 (br m, 8H, CH_2), 2.04 (s, 12H, CH_3), 1.95 (br m, 8H, CH_2), 1.62 (br m, 8H, CH_2), 1.49-1.21 (m, masked by heptane, CH_2), 0.91 (m, masked by heptane, CH_3) ppm. MALDI-TOF MS : *m/z* 1442.8 calcd for $C_{94}H_{111}BMg_2N_8O_2$, 1442.8 ($M^{+\bullet}$). ESI HRMS : *m/z* 1443.8654 calcd for $C_{94}H_{111}BMg_2N_8O_2$, 1443.8746 ($M+H^+$). UV-vis (THF) λmax (log ε)= 408 (5.58), 569 (4.04), 614 (3.85) nm.

Magnesium(II) 5-{8-[magnesium(II)-10,20-dinonylporphyrin-5-yl]-biphenylene-1-yl}-15-[4-{10,20-bis-3,5-di-tert-butyl-phenyl)-porphyrin-5-yl}phenyl]-10,20-dinonylporphyrin 1

Under an inert atmosphere, a solution of $Pd_2(dba)_3$ (0.9 mg, 0.001 mmol) and *S*-PHOS (2.5 mg, 0.006 mmol) in 6 mL of freshly distilled toluene was added onto a mixture of magnesium(II) 5-{8-[magnesium(II)-10,20-dinonylporphyrin-5-yl]-biphenylene-1-yl}-15-(4,4,5,5-tetramethyl-[1,3,2] dioxaborolan-2-yl)-10,20-dinonylporphyrin (15 mg, 0.010 mmol), 5-(4-bromophenyl)-10,20-bis-(3,5-di-tert-butyl-phenyl)-porphyrin (13 mg, 0.015 mmol) and cesium carbonate (13 mg, 0.04 mmol). 3 mL of anhydrous DMF was added and the reaction mixture was stirred at 90 °C for 16 h. The reaction was quenched with 10 ml of water. The organic layer was separated, extracted from aqueous phase. The combined organic fractions were washed with brine (2 x 20 mL) and dried over $MgSO_4$. The solvents were removed under vacuum and the purple residue was purified over SEC chromatography affording the title compound as a dark purple solid (6 mg, 28%). ^{1}H NMR (300.16 MHz, THF-d^8): δ 10.41 (s, 1H, *meso*), 9.83 (dd, 1H, *J* =7.0 Hz, *J* =1.7 Hz, C_6H_4), 9.56 (d, 2H, *J* = 4.6 Hz, β), 9.50 (d, 2H, *J* = 4.1 Hz, β), 9,39 (s, 1H, *meso*), 9.24 (d, 2H, *J* = 4.4 Hz, β), 9.14 (d, 2H, *J* = 4.2 Hz, β), 9.11 (dd, 1H, *J* =7.0 Hz, *J* =1.9 Hz, C_6H_4), 8,99 (d, 2H, *J* = 4.2 Hz, β), 8.90 (d, 2H, *J* = 3.9 Hz, β), 8.79 (d, 2H, *J* = 3.9 Hz, β), 8.62 (d, 2H, *J* = 4.7 Hz, β), 8.52 (d, 3H, *J* = 4.0 Hz, β + C_6H_3), 8.46 (dd, 1H, *J* =7.0 Hz, *J* =1.9 Hz, C_6H_4), 8.39 (s, 2H, C_6H_3), 8.31 (s, 2H, C_6H_3), 8.24 (d, 2H, *J* = 4.7 Hz, β), 8.03 (t, 2H, *J* =1.8 Hz, C_6H_3), 7.97 (d, 2H, *J* = 5.4 Hz, β), 7.44 (d, 1H, *J* =7.2 Hz, DPB), 7.30 (d, 1H, *J* =6.6 Hz, DPB), 7.24 (dd, 1H, *J* =2.8 Hz, *J* =7.8 Hz, DPB), 7.21 (dd, 1H, *J* =2.1 Hz, *J* =8.1 Hz, DPB), 7.05 (m, 2H, DPB), 3.58 (masked by THF-d^8), 3.46 (m, 8H, CH_2), 2.01 (m, 8H, CH_2), 1.66 (s, 18H, tBu), 1.34 (m, masked by water and heptane, CH_2), 1.29 (s, 18H, tBu), 0.90 (m, masked by heptane, CH_3) and -2.60 (s, 2H, NH) ppm. MALDI-TOF MS : *m*/*z* 2079.2 calcd for $C_{142}H_{156}Mg_2N_{12}$, 2079.2 ($M^{+\bullet}$). ESI HRMS : *m*/*z* 2079.2318 calcd for $C_{142}H_{156}Mg_2N_{12}$, 2079.2344 ($M^{+\bullet}$). UV-vis (THF) λmax (log ε)= 417 (5.65), 509 (4.32), 544 (4.10), 572 (4.10), 583 (4.13), 615 (3.99), 640 (3.92) nm.

Instruments. ^{1}H NMR spectra were recorded on a Bruker Avance II 300 (300 MHz) spectrometer at the "Plateforme d'Analyse Chimique et de Synthèse Moléculaire de l'Université de Bourgogne (PACSMUB)"; chemical shifts are expressed in ppm relative to chloroform (7.26 ppm), methylene chloride (5.30 ppm) or THF-d^8 (1.73 and 3.58 ppm). UV-vis spectra were recorded on a Varian Cary 1 spectrophotometer. Mass spectra and accurate

mass measurements (HR-MS) were obtained respectively on a Bruker Daltonics Ultraflex II spectrometer in the MALDI/TOF reflectron mode using dithranol as a matrix and on a Bruker MicroQTof instrument or on a Thermo LTQ Orbitrap XL mass spectrometer in the positive ESI mode. Both measurements were performed at the "Plateforme d'Analyse Chimique et de Synthèse Moléculaire de l'Université de Bourgogne (PACSMUB)". UV-visible spectra were recorded on a Hewlett-Packard diode array model 8452A and the emission spectra were obtained using a double monochromator Fluorolog 2 instrument from Spex. The fluorescence lifetimes were measured using a TimeMaster Model TM-3/2003 apparatus from PTI. The source was nitrogen laser with high-resolution dye laser (fwhm ~1600ps) and fluorescence lifetimes were obtained from deconvolution or distribution lifetimes analysis.

Transient absorption spectroscopy. The fs transient absorption spectra (at 1.5 nm of spectra resolution) along with the decay traces were acquired with a Helios spectrometer from Ultrafast Systems in the 450-800 nm range and 150 fs to 3.0 ns time window. This Helios instruments used an all-reflective supercontinuum generation setup resulting in a temporal chirp of the probe pulse of ~200 fs. Fiber optics were used to couple the multichannel spectrometer with a CMOS sensor with 1.5 nm intrinsic resolution. The instrument control and the data acquisition were made with a LabVIEW-based software. The data analysis was made with the Surface Xplorer^{TM} software package. The laser excitation was performed using the Solstice (Spectra-Physics), a one box ultrafast regenerative Ti-sapphire amplifier. The system produced pulses centered at 795nm with bandwidth of ~15nm, energy of 3.75mJ, ~75 fs duration and 1 kHz repetition rate. The frequency was doubled with a second harmonic generator crystal (BBO) to obtain an excitation at 400 nm.

Computations. All density functional theory (DFT) and time dependent density functional theory (TD-DFT) calculations were performed with Gaussian 09[3] at the Université de Sherbrooke with the Mammouth supercomputer supported by *Le Réseau Québécois De Calculs Hautes Performances*. The DFT geometry optimisations as well as TD-DFT calculations[4-13] were carried out using the B3LYP method. 6-31g* basis sets for all porphyrin macrocycles, the biphenylene linkage as well as the bridging benzene were used. 3-21g* basis sets for solubilising side groups[14-18] were employed. 6-31g* basis sets were used for magnesium atoms.[14-19]

Quantum yields. The fluorescence quantum yields were measured against H_2TPP tetraphenylporphyrin in 2MeTHF (Φ_F = 0.11 in 2MeTHF at 296K).[20] Each measurement was performed 3 times with fresh solutions.

2. References

1. M. Filatov, F. Laquai, D. Fortin, R. Guilard, P. D. Harvey, *Chem. Commun.* 2010, **46,** 9176.

2. C. Maeda, S. Yamaguchi, C. Ikeda, H. Shinokubo, and A. Osuka, *Org. Lett.* 2008, **10**, 549.

3. M. J. Frisch, *et al. Gaussian, Inc., Wallingford CT*, 2004.

4. P. Hohenberg and W. Kohn, *Phys. Rev.* 1964, **136**, B864–871.

5. P. Hohenberg and W. Kohn, W. *J. Phys. Rev.* 1965, **140**, A1133–1138.

6. R. G. Parr, and W. Yang, *Density-functional theory of atoms and molecules*, Oxford Univ. Press: Oxford, 1989.

7. D. R. Salahub and M. C. Zerner, *The Challenge of d and f Electrons, Amer. Chem. Soc. Washington, D.C.* 1989.

8. R. Bauernschmitt and R. Ahlrichs, *Chem. Phys. Lett.* 1996, **256**, 454.

9. M. E. Casida, C. Jamorski, K. C. Casida, and D. R. Salahub, *J. Chem. Phys.* 1998, **108**, 4439.

10. R. E. Stratmann, G. E. Scuseria, and M. J. Frisch, *J. Chem. Phys.* 1998, **109**, 8218.

11. C. Lee, and W. Yang, and R. G. Parr, *Phys. Rev. B* 1988, **37**, 785.

12. B. Miehlich, A. Savin, H. Stoll, and H. Preuss, H. *Chem. Phys. Lett.* 1989, **157**, 200.

13. A. D. Becke, *J. Chem. Phys.* 1993, **98**, 5648.

14. Binkley, J. S.; Pople, J. A.; Hehre, W. J. *J. Am. Chem. Soc.* 1980, **102**, 939.

15. M. S. Gordon, J. S. Binkley, J. A. Pople, W. J. Pietro, and W. J. Hehre, *J. Am. Chem. Soc.* 1982, **104**, 2797.

16. W.J. Pietro, M. M. Francl, W.J. Hehre, D. J. Defrees, J. A. Pople, and J. S. Binkley, *J. Am. Chem. Soc.* 1982, **104**, 5039.

17. K. D. Dobbs and W. J. Hehre, *J. Comput. Chem.* 1986, **7**, 359.

18. K. D. Dobbs and W. J. Hehre, *J. Comput. Chem.* 1987, **8**, 861.

19. K. D. Dobbs and W. J. Hehre, *J. Comput. Chem.* 1987, **8**, 880.

20. S. Gentermann, N. Y. Nelson, L. Jaquind, D. J. Nurco, S. H. Leung, G. J. Medforth, K. M. Smith, F. Fajer, D. Leung, J. Phys. Chem. B. 1997, **101**, 1247.

3. NMR and High Resolution Mass Spectra

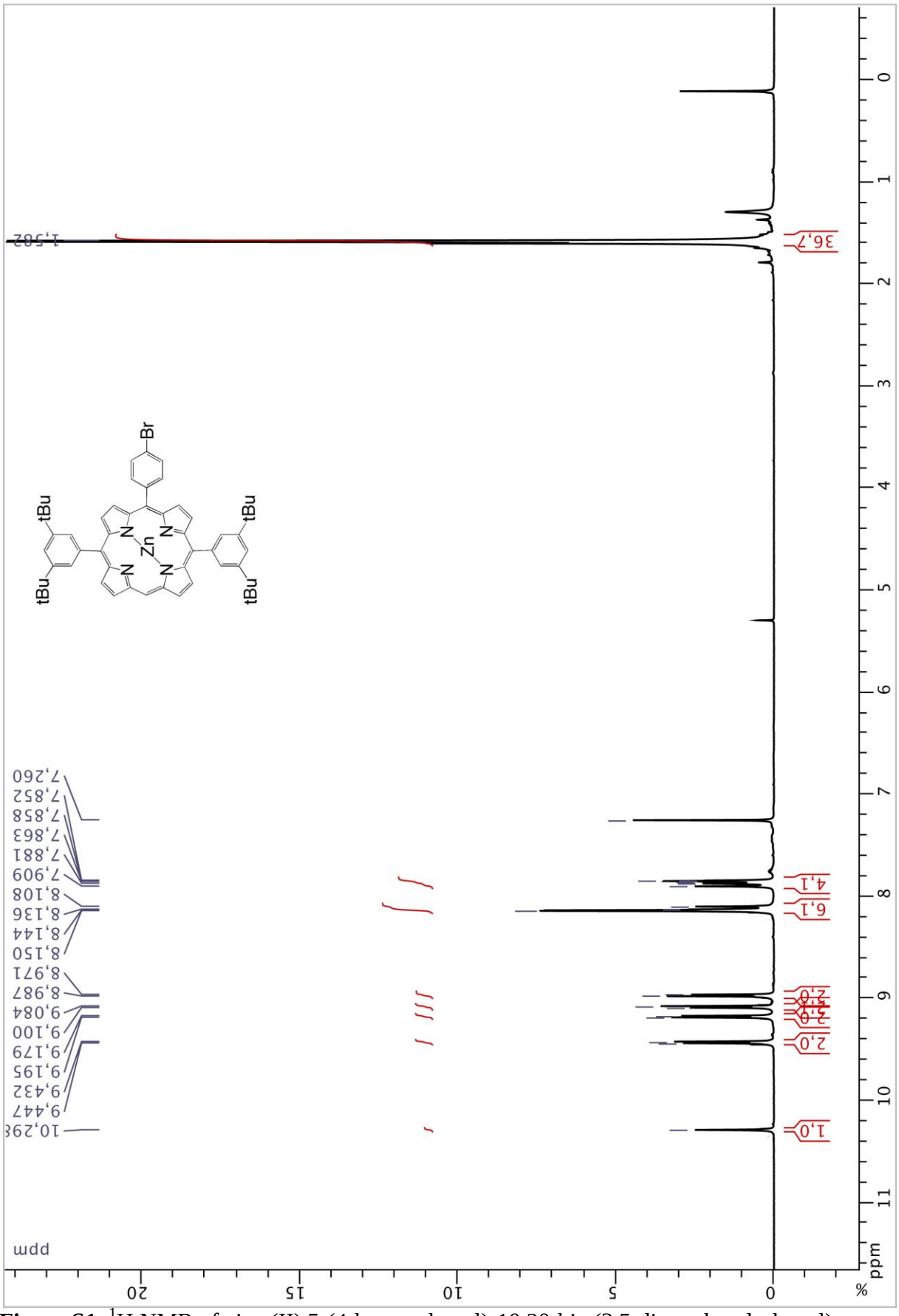

Figure S1. ^{1}H NMR of zinc (II) 5-(4-bromophenyl)-10,20-bis-(3,5-di-tert-butyl-phenyl)-porphyrin **7** (300 MHz, $CDCl_3$)

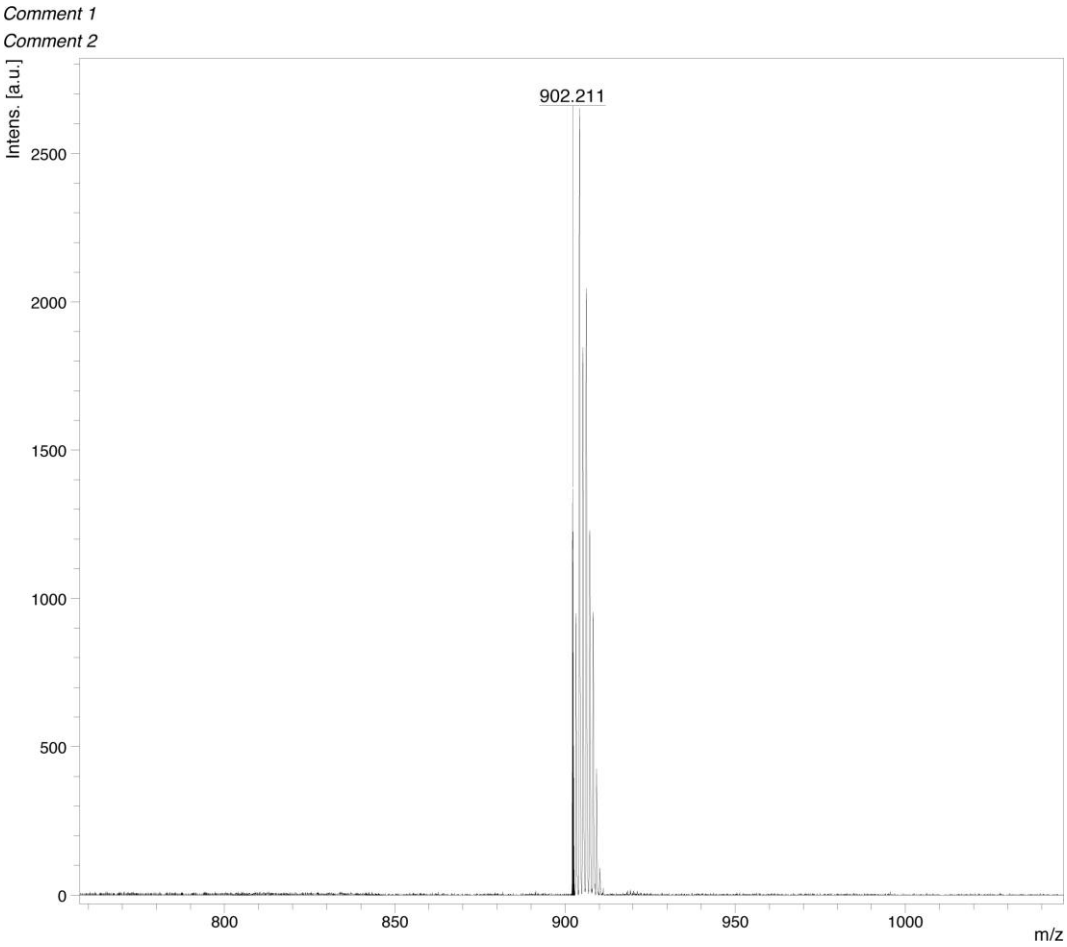

Figure S2. MALDI-TOF spectrum of **7** (positive mode)

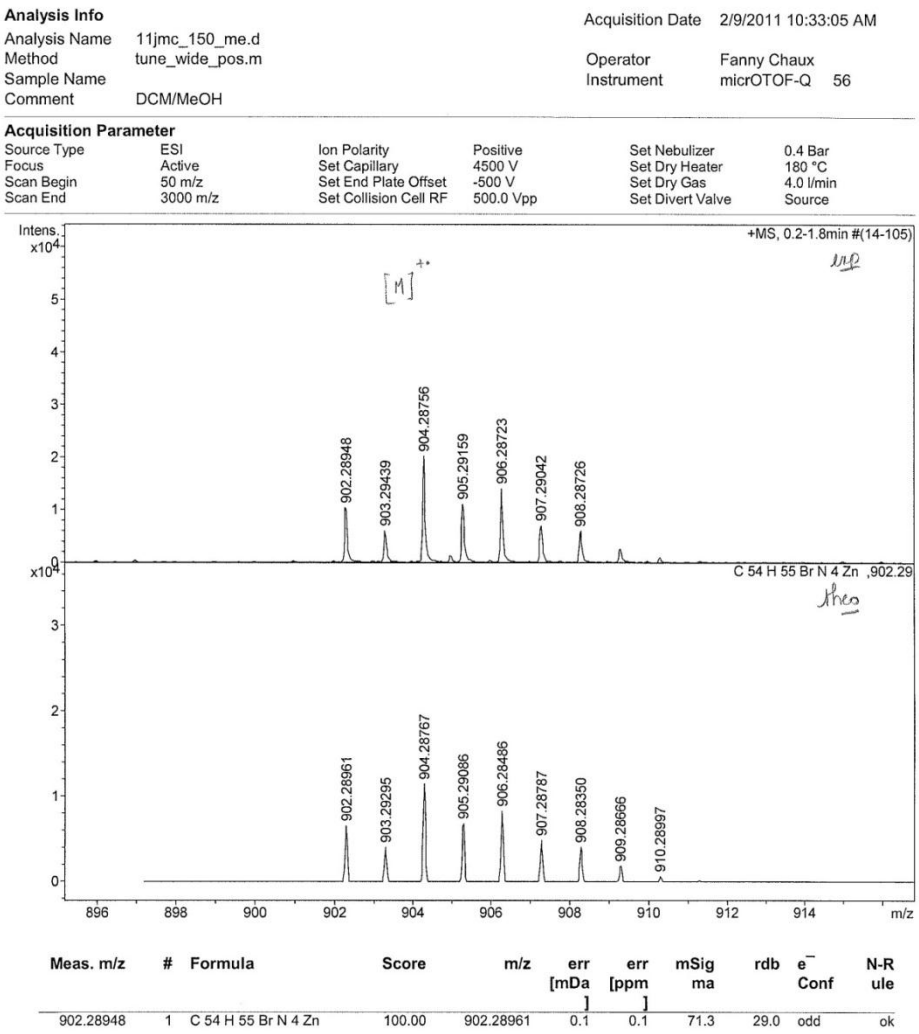

Meas. m/z	#	Formula	Score	m/z	err [mDa]	err [ppm]	mSigma	rdb	e⁻ Conf	N-Rule
902.28948	1	C 54 H 55 Br N 4 Zn	100.00	902.28961	0.1	0.1	71.3	29.0	odd	ok

Figure S3. ESI HRMS spectrum of **7** (positive mode)

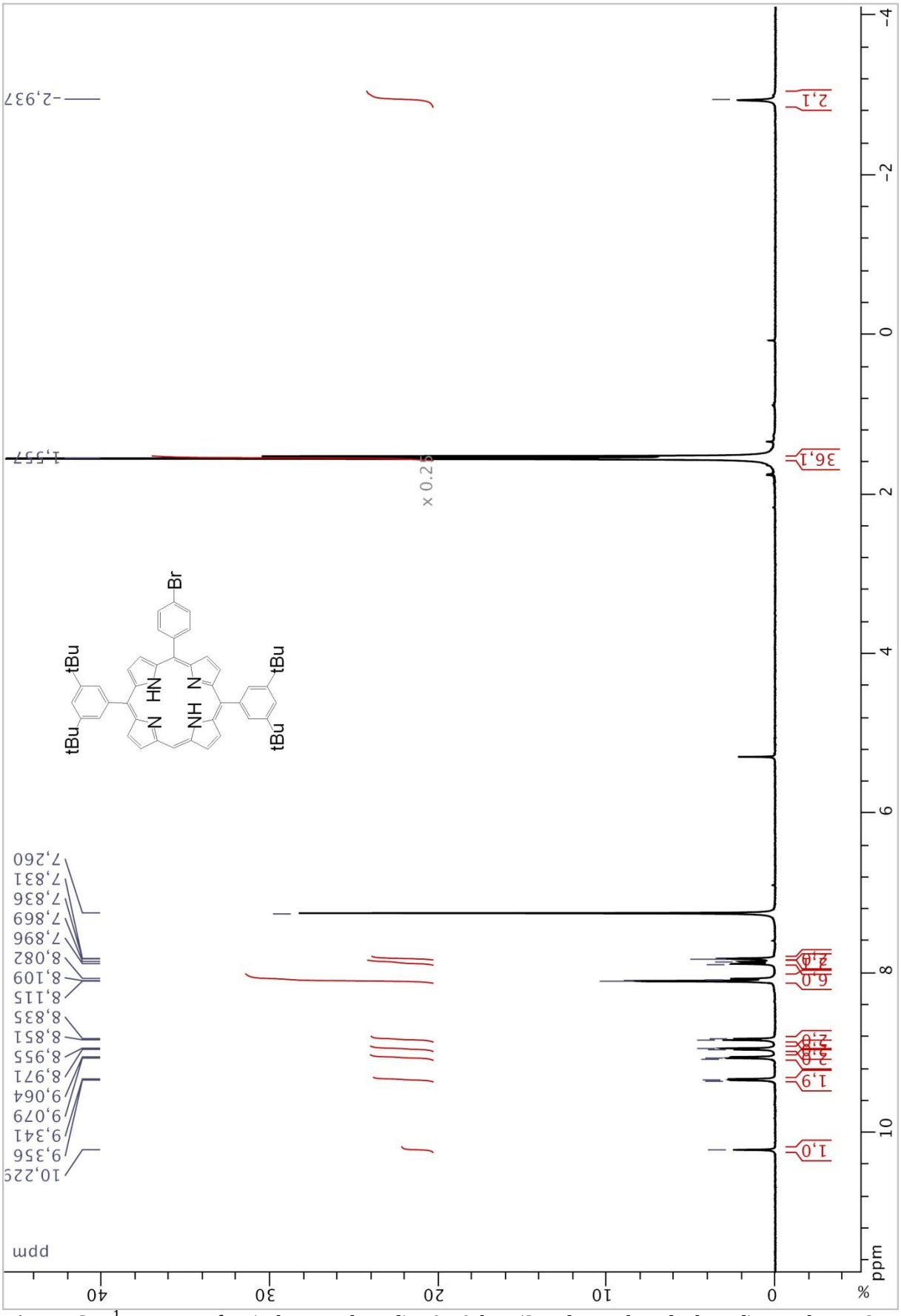

Figure S4. ^{1}H NMR of 5-(4-bromophenyl)-10,20-bis-(3,5-di-tert-butyl-phenyl)-porphyrin **8** (300 MHz, $CDCl_3$).

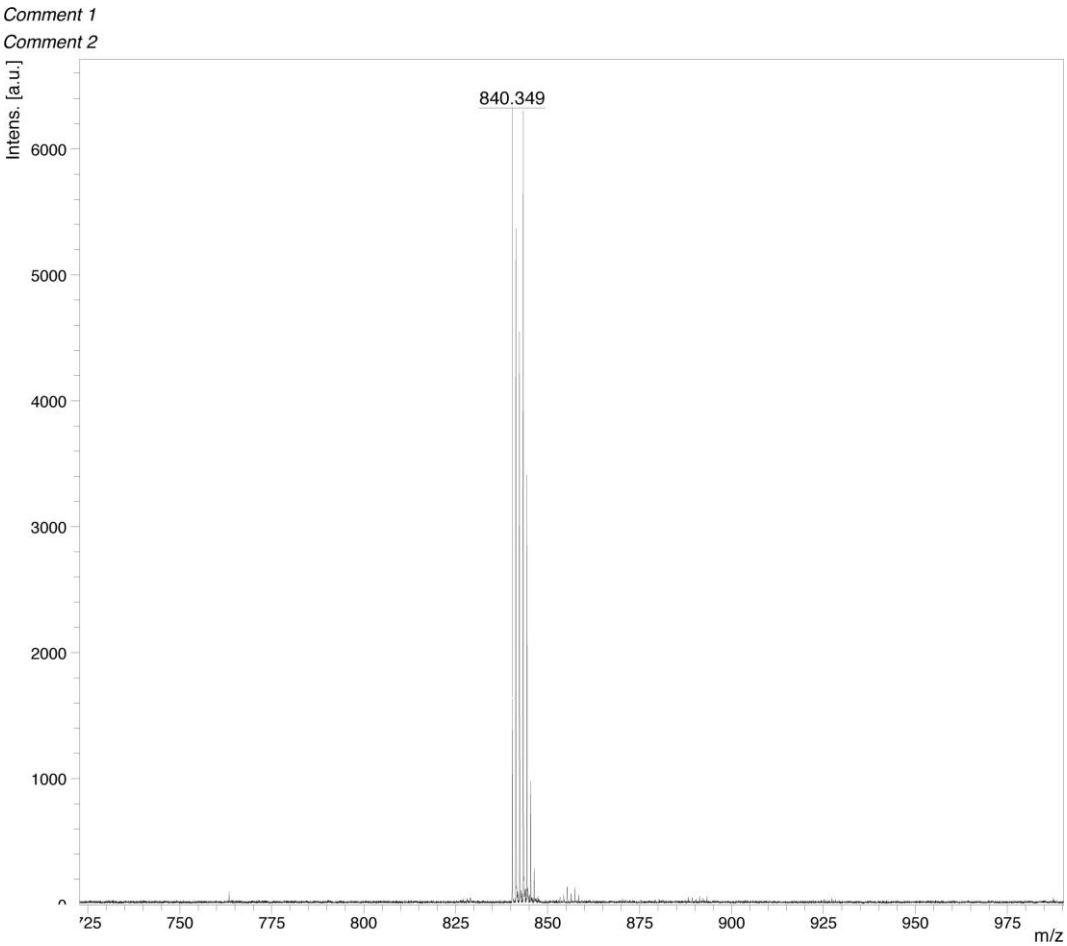

Figure S5. MALDI-TOF spectrum of **8** (positive mode)

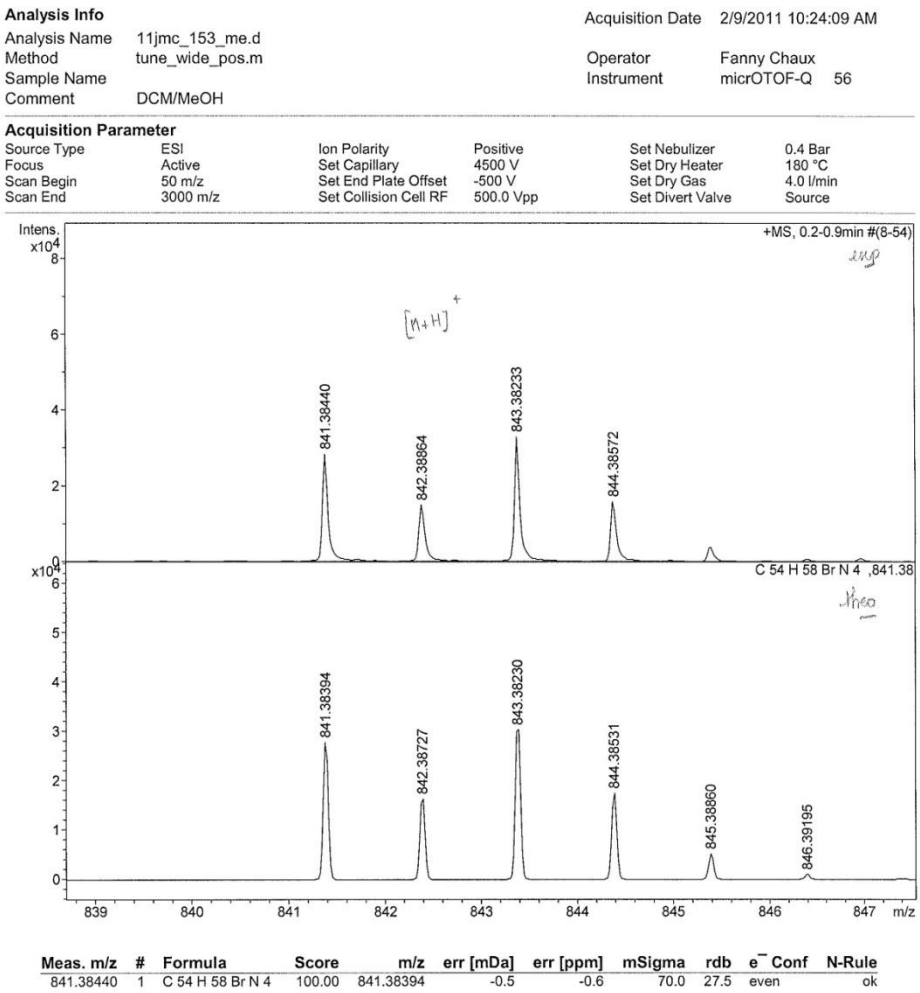

Meas. m/z	#	Formula	Score	m/z	err [mDa]	err [ppm]	mSigma	rdb	e⁻ Conf	N-Rule
841.38440	1	C 54 H 58 Br N 4	100.00	841.38394	-0.5	-0.6	70.0	27.5	even	ok

Figure S6. ESI HRMS spectrum of **8** (positive mode)

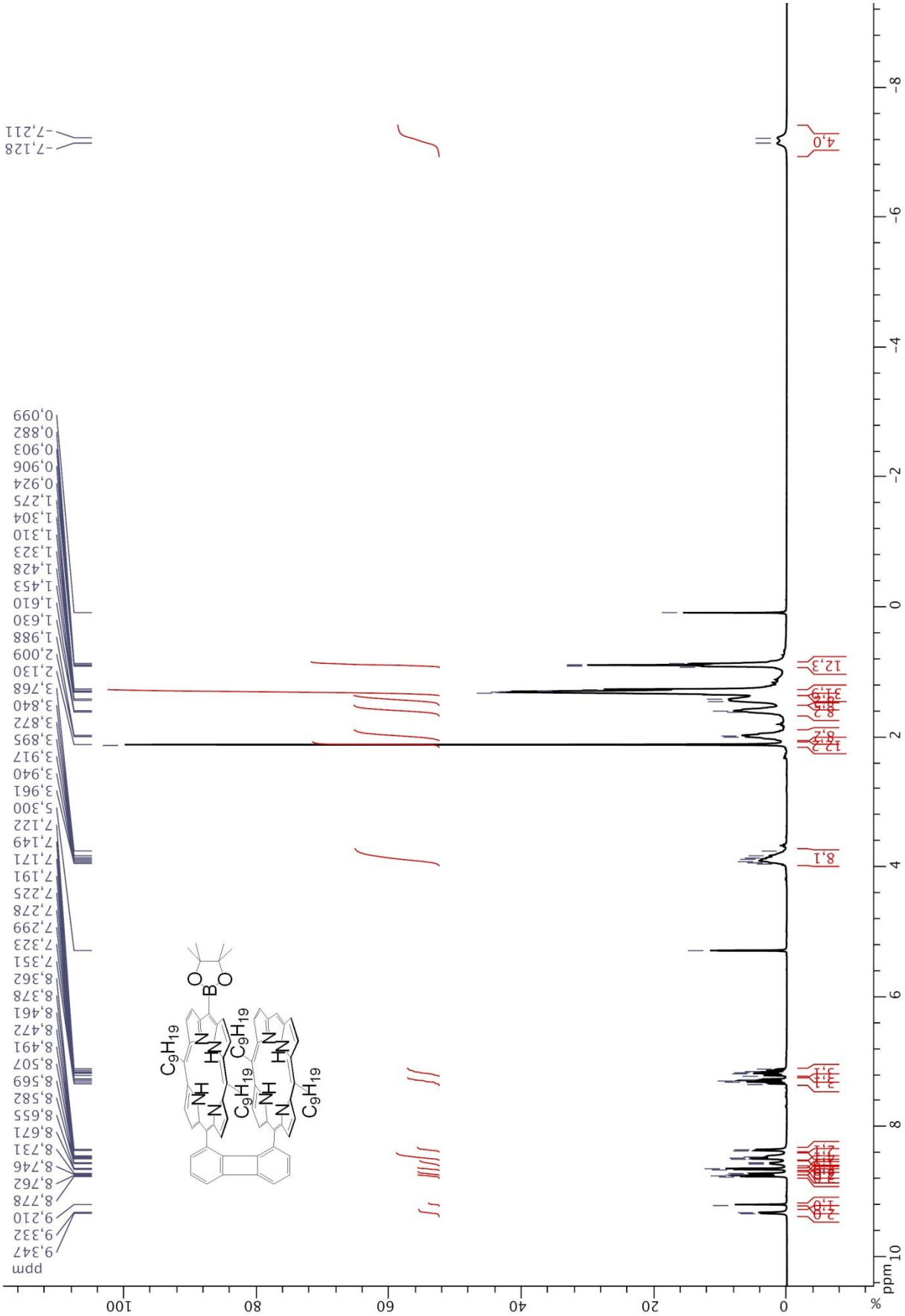

Figure S7. ^{1}H NMR of 5-{8-[10,20-dinonylporphyrin-5-yl]-biphenylene-1-yl}-15-(4,4,5,5-tetramethyl-[1,3,2]-dioxaborolan-2-yl)-10,20-dinonylporphyrin **12** (300 MHz, CD_2Cl_2)

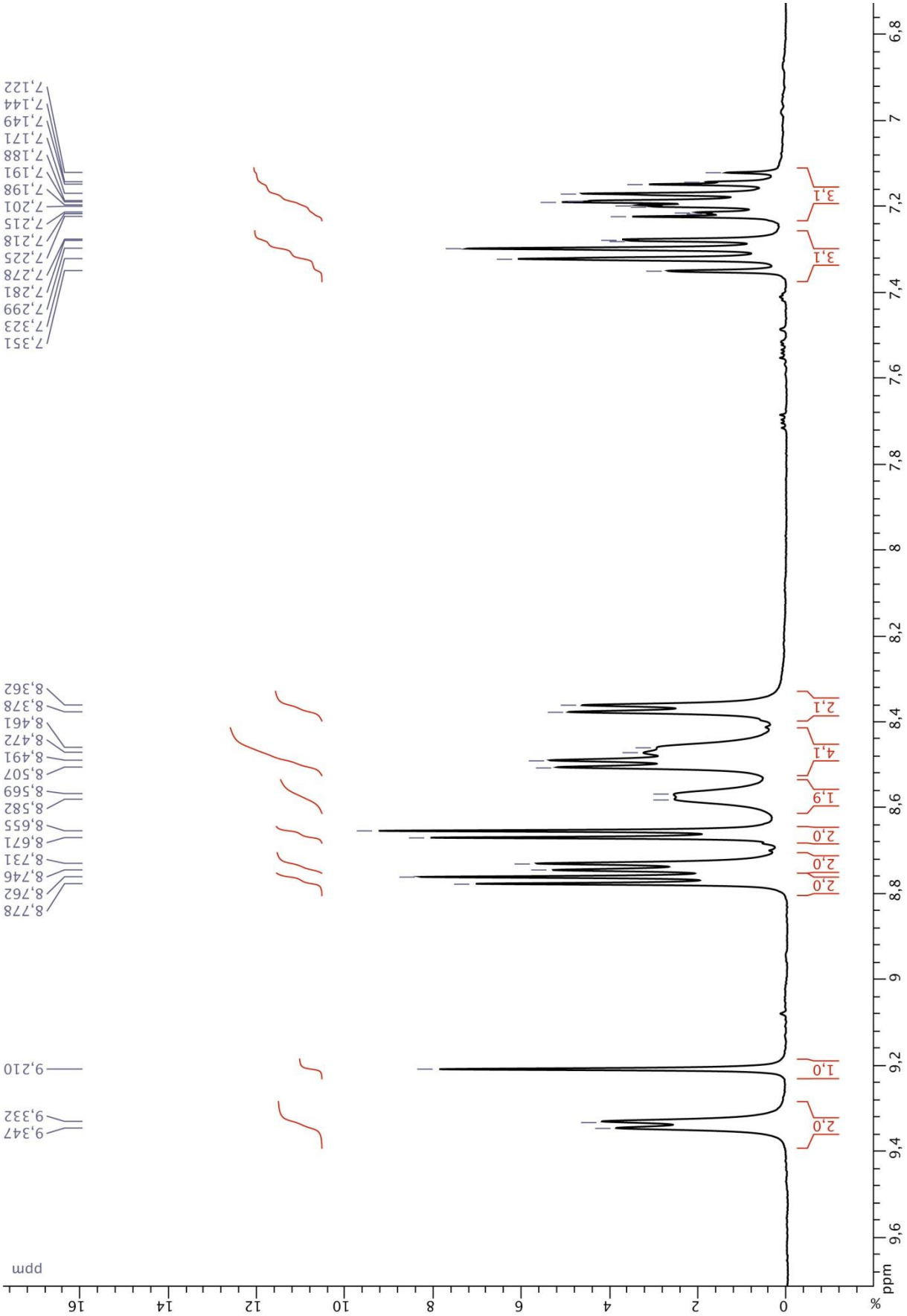

Figure S8. Aromatic part of ^{1}H NMR of **12** (300 MHz, CD_2Cl_2)

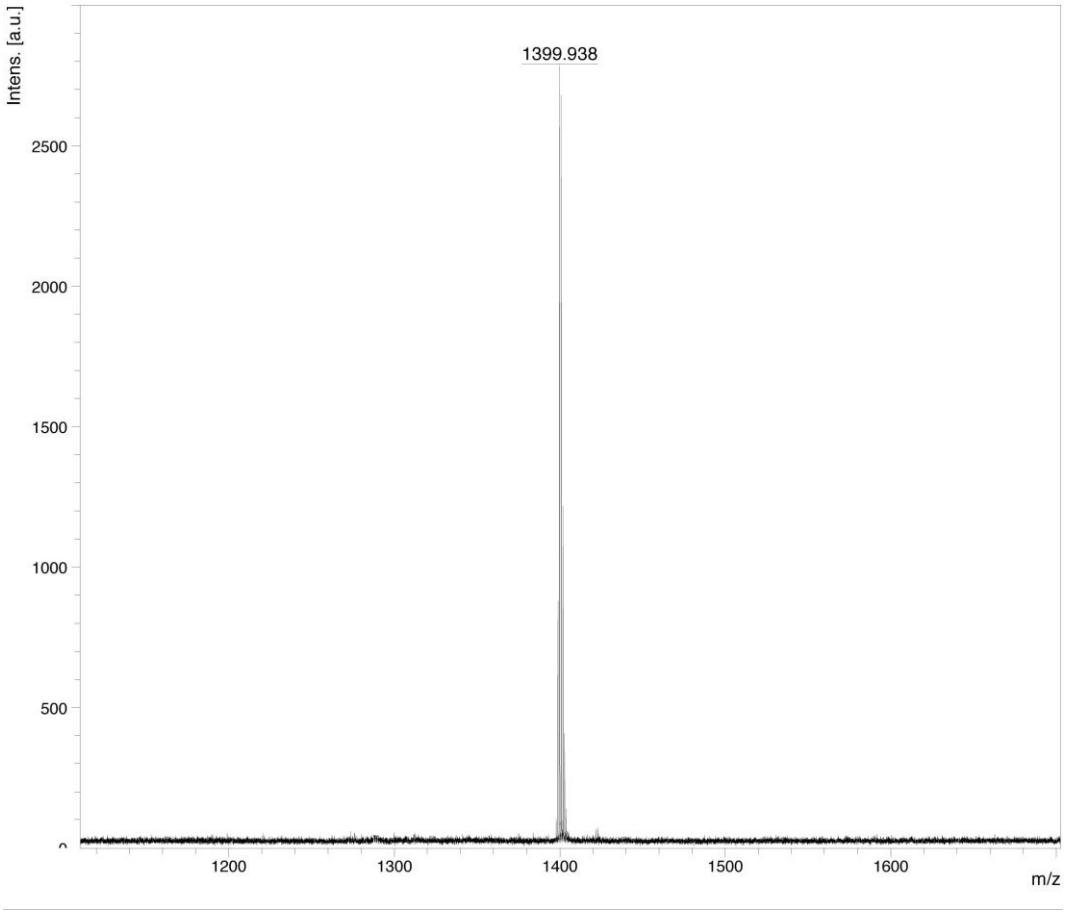

Figure S9. MALDI-TOF spectrum of **12** (positive mode)

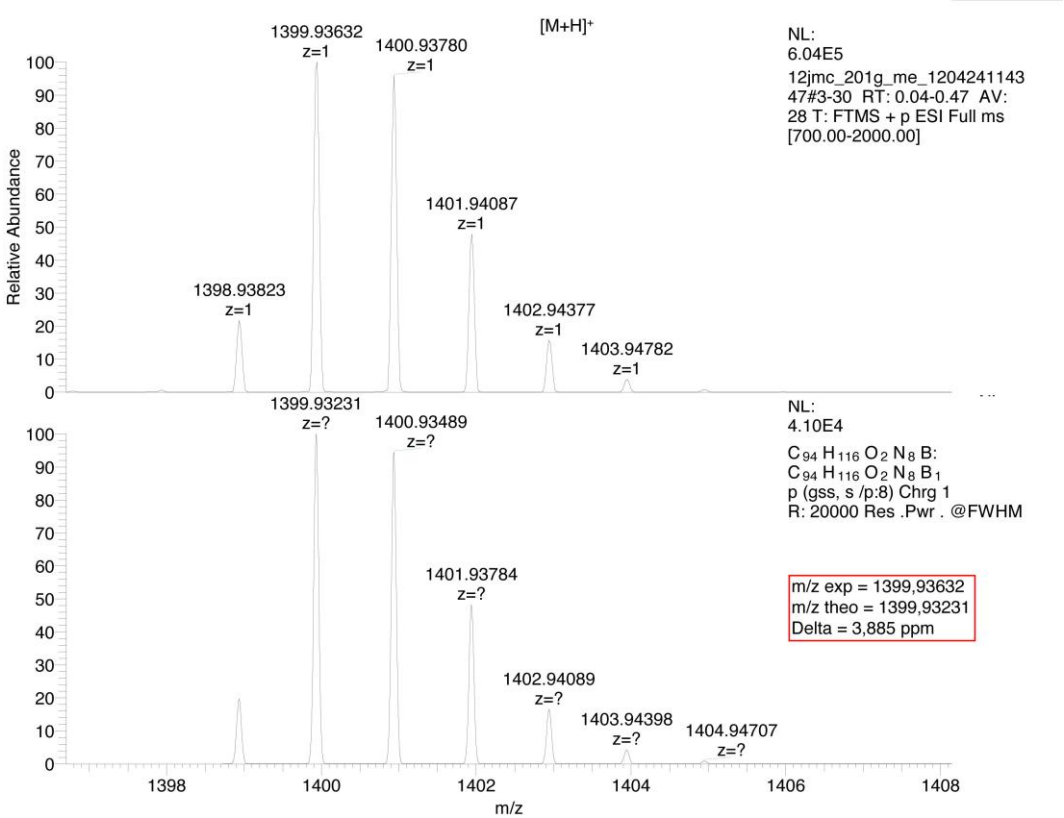

Figure S10. ESI HRMS spectrum of **12** (positive mode)

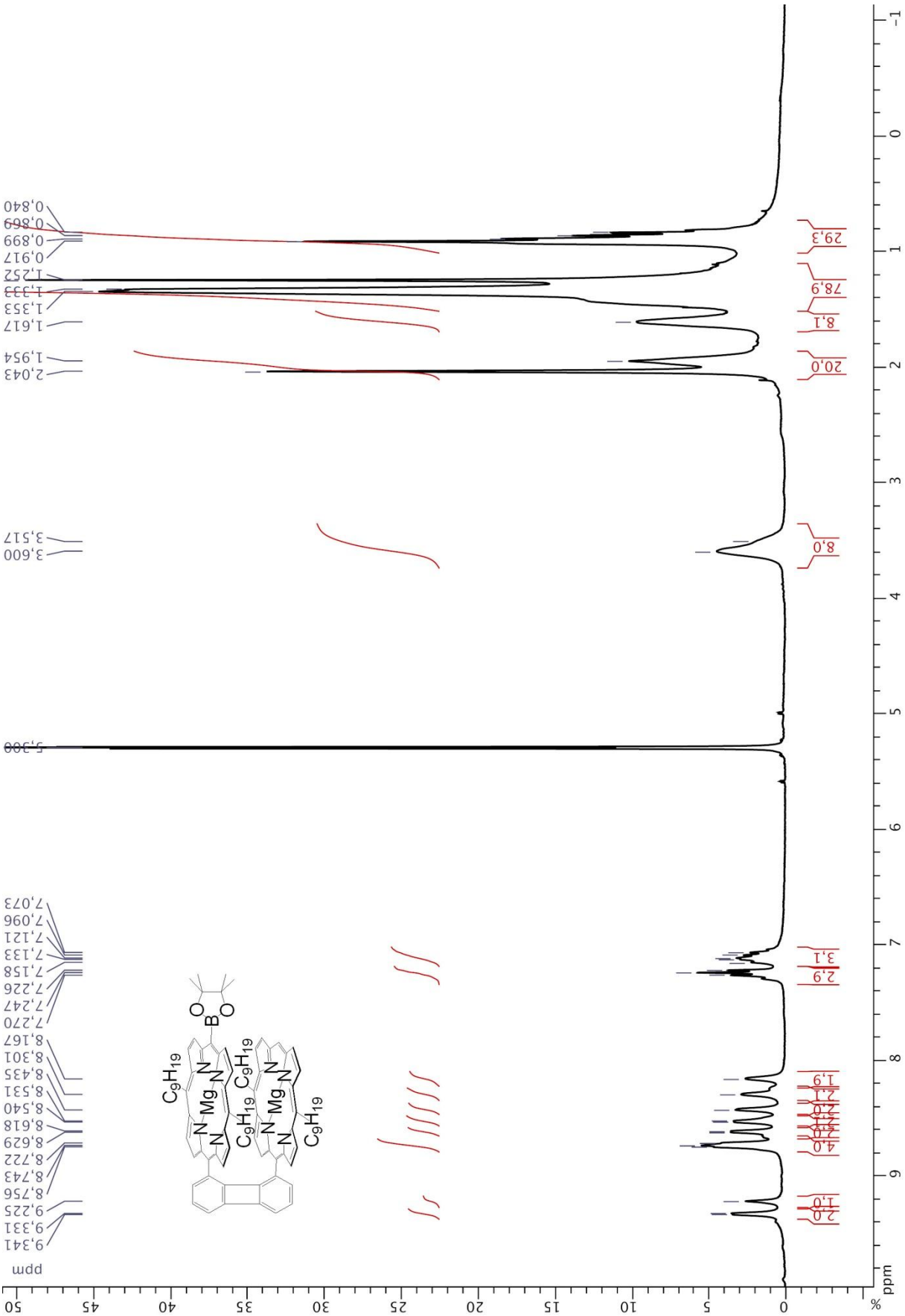

Figure S11. ^{1}H NMR of magnesium(II) 5-{8-[magnesium(II)-10,20-dinonylporphyrin-5-yl]-biphenylene-1-yl}-15-(4,4,5,5-tetramethyl-[1,3,2] dioxaborolan-2-yl)-10,20-dinonylporphyrin **13** (300 MHz, CD_2Cl_2)

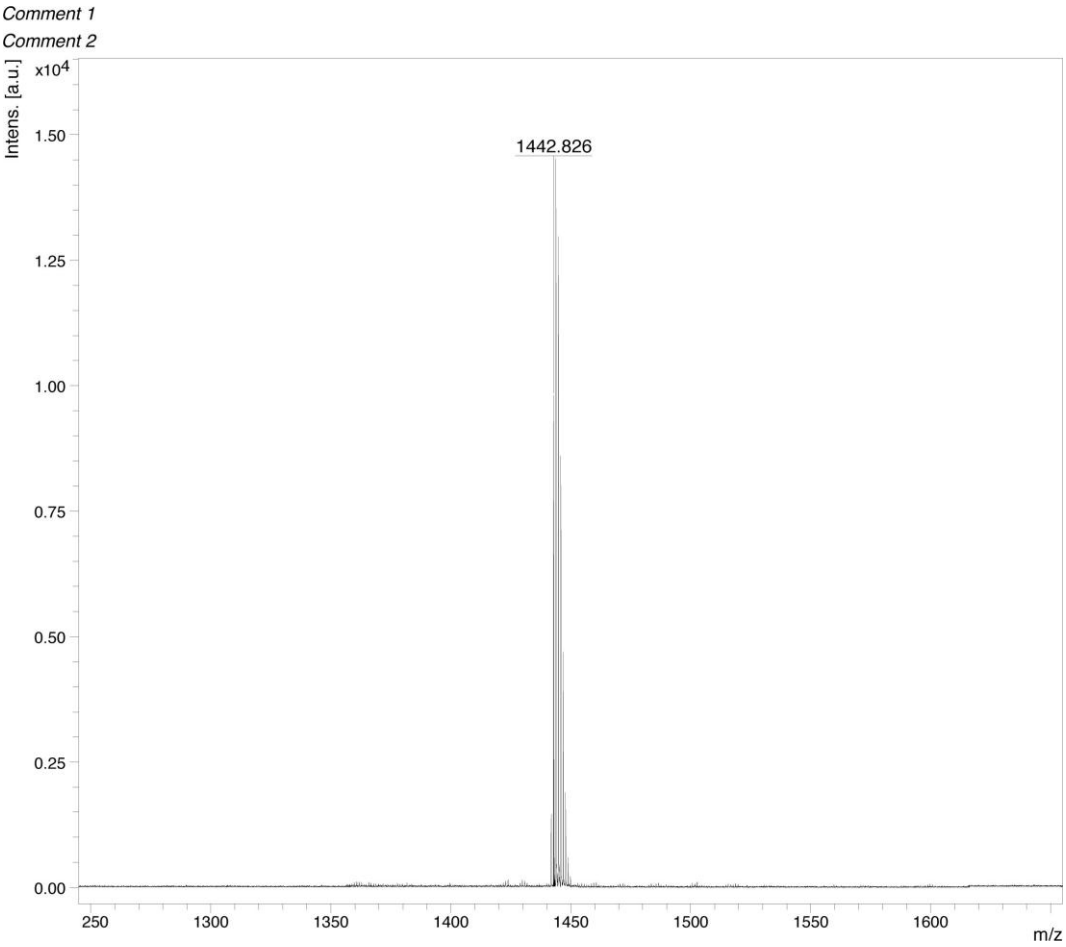

Figure S12. MALDI-TOF spectrum of **13** (positive mode)

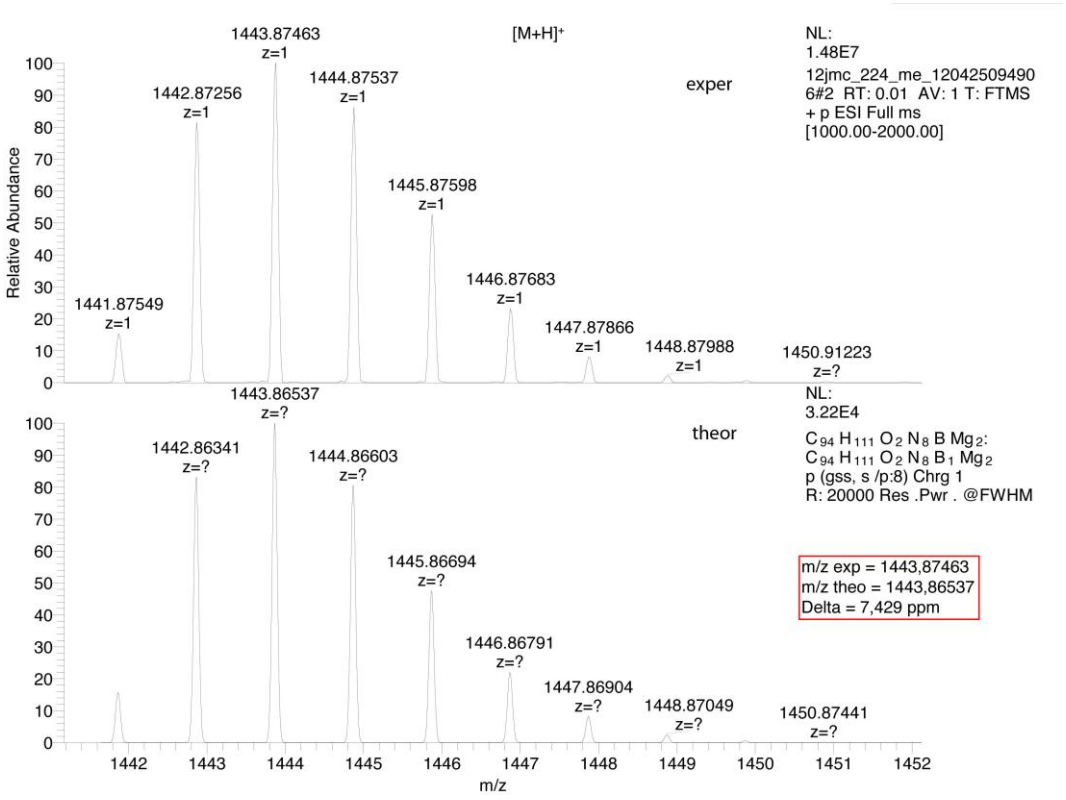

Figure S13. ESI HRMS spectrum of **13** (positive mode)

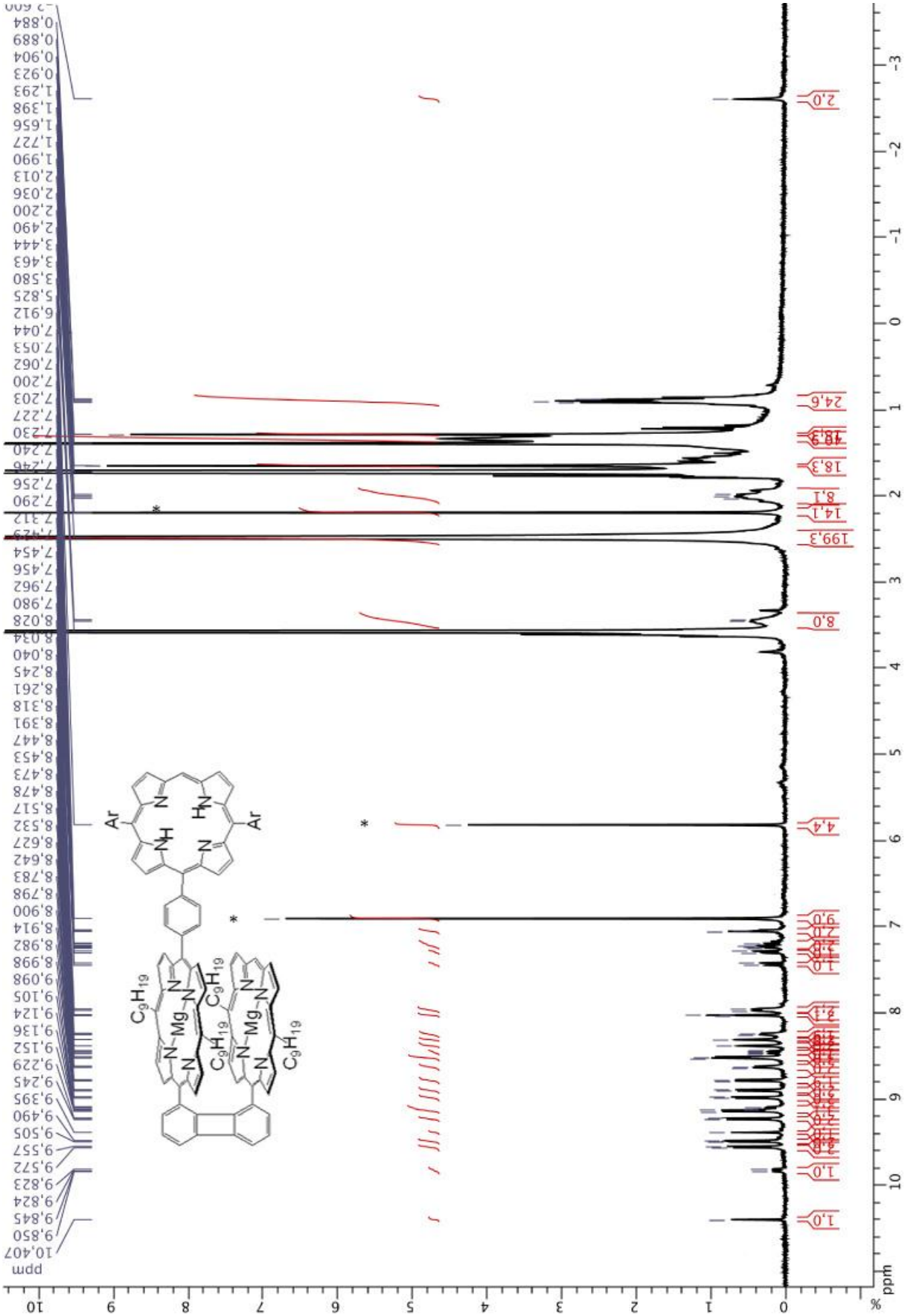

Figure S14. ^{1}H NMR of Magnesium(II) 5-{8-[magnesium(II)-10,20-dinonylporphyrin-5-yl]-biphenylene-1-yl}-15-[4-{10,20-bis-3,5-di-tert-butyl-phenyl)-porphyrin-5-yl}phenyl]-10,20-dinonyl-porphyrin **1**(300 MHz, THF-d^{8}) *2,6-dimethyl,4-tert-butylphenol

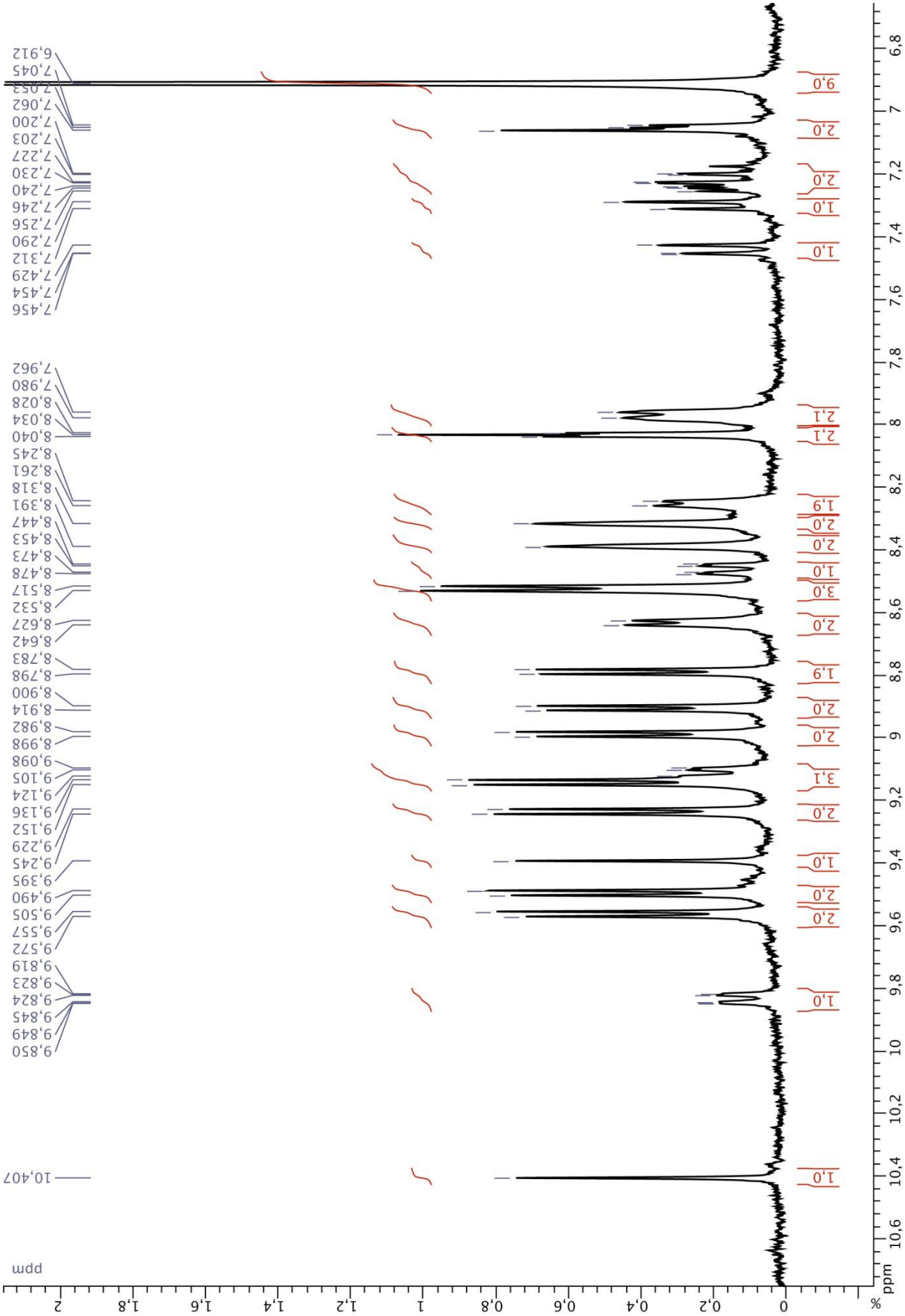

Figure S15. Aromatic part of ^{1}H NMR of **1** (300 MHz, THF-d^{8})

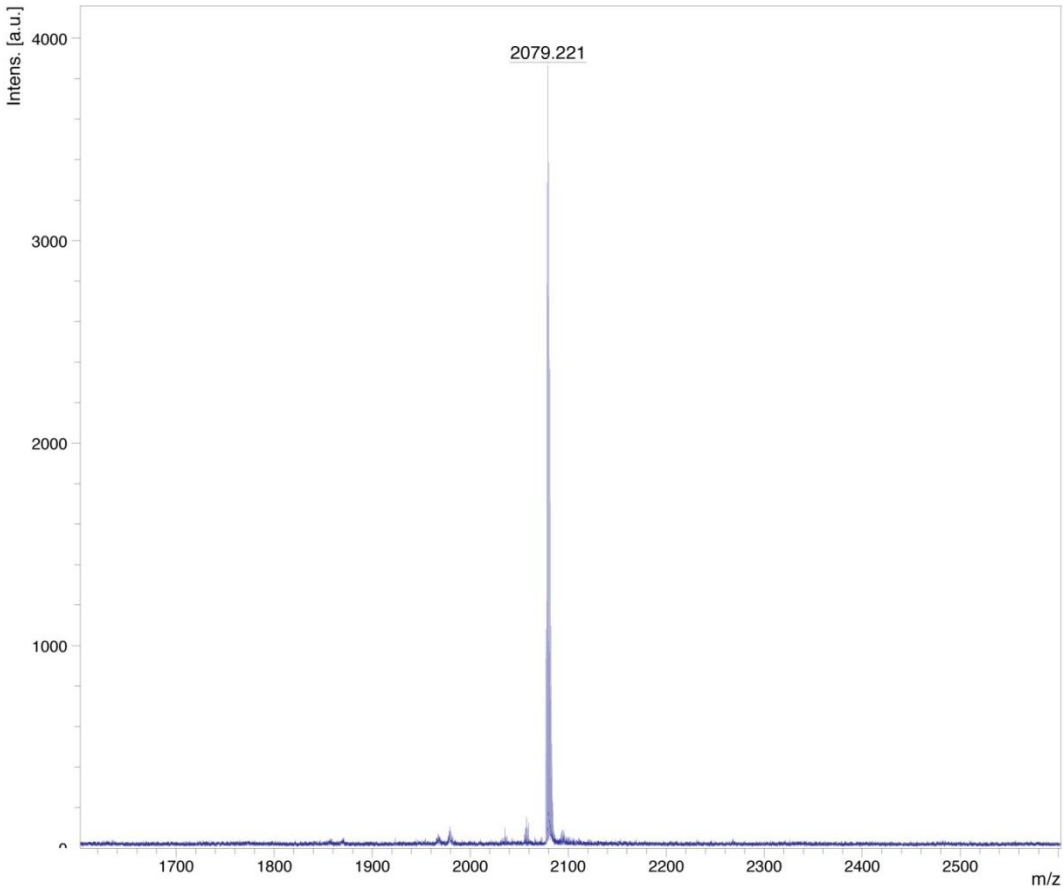

Figure S 16. MALDI-TOF spectrum of **1** (positive mode)

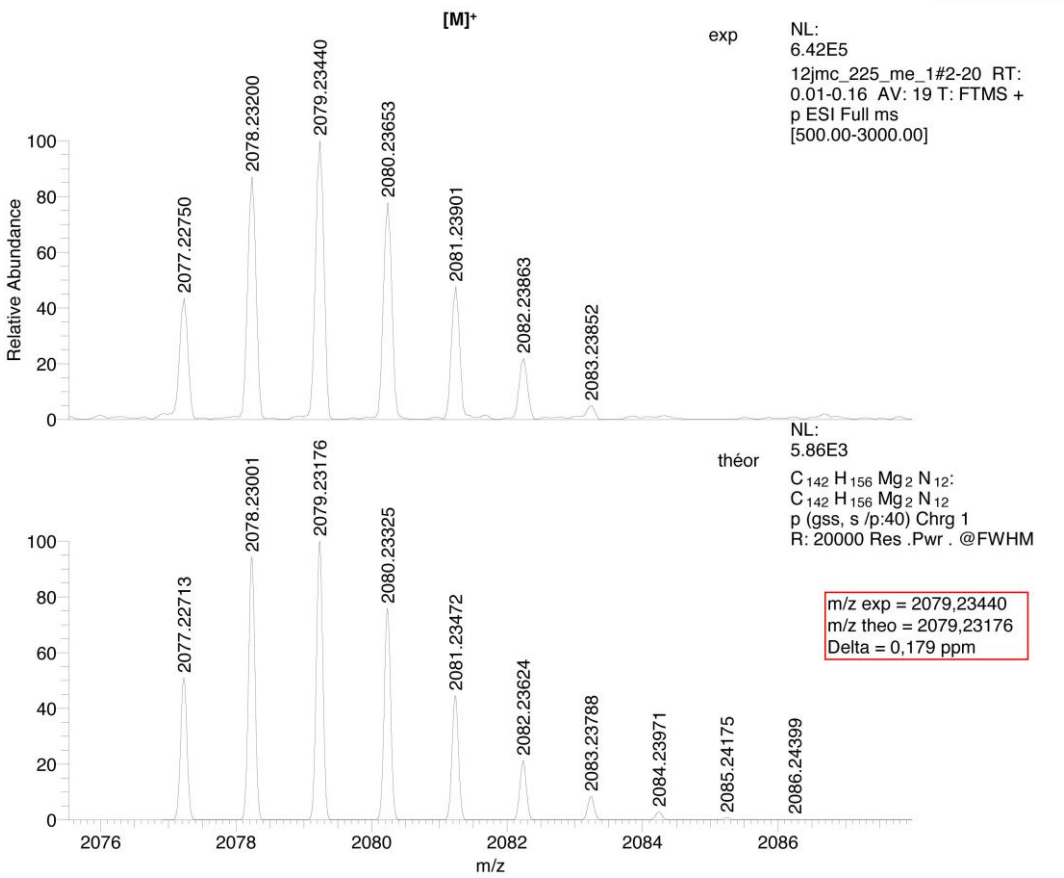

Figure S17. ESI HRMS spectrum of **1** (positive mode)

4. Optical spectra

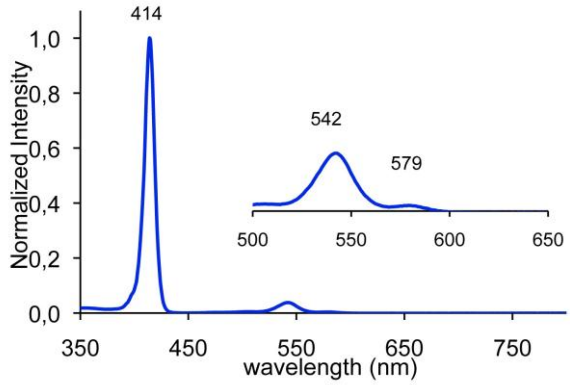

Figure S 20. Absorption spectrum of **7** in THF

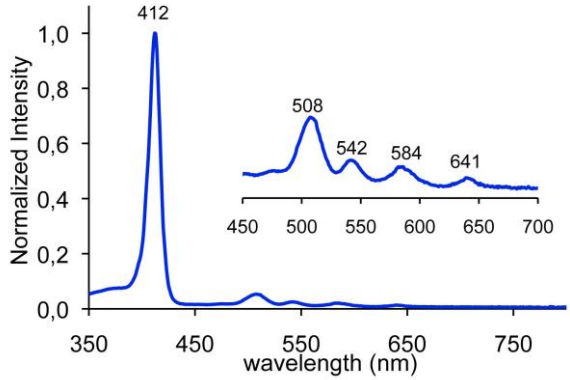

Figure S 18. Absorption spectrum of **8** in THF

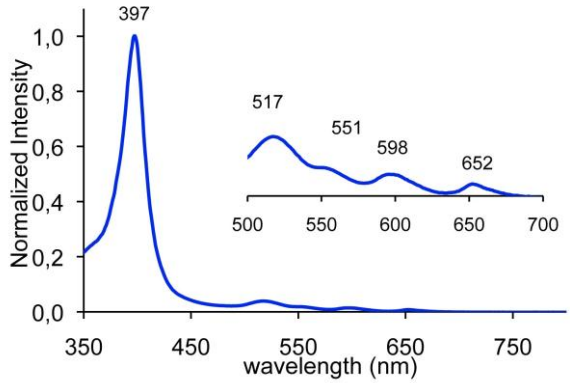

Figure S19. Absorption spectrum of **12** in THF

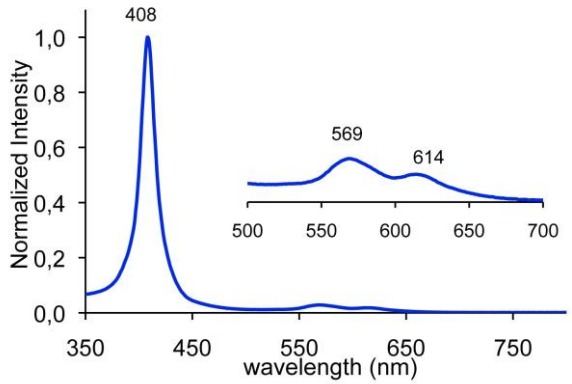

Figure S 20. Absorption spectrum of **13** in THF

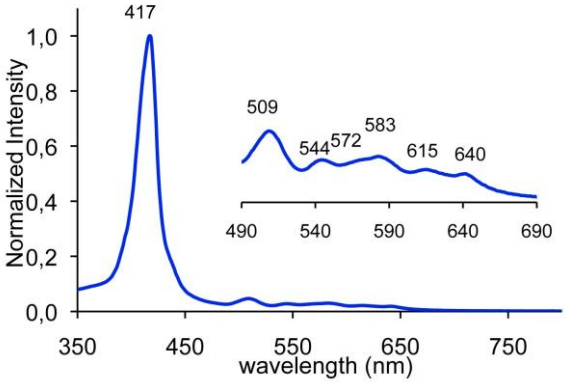

Figure S 21. Absorption spectrum of **1** in THF

5. Computed energy barriers

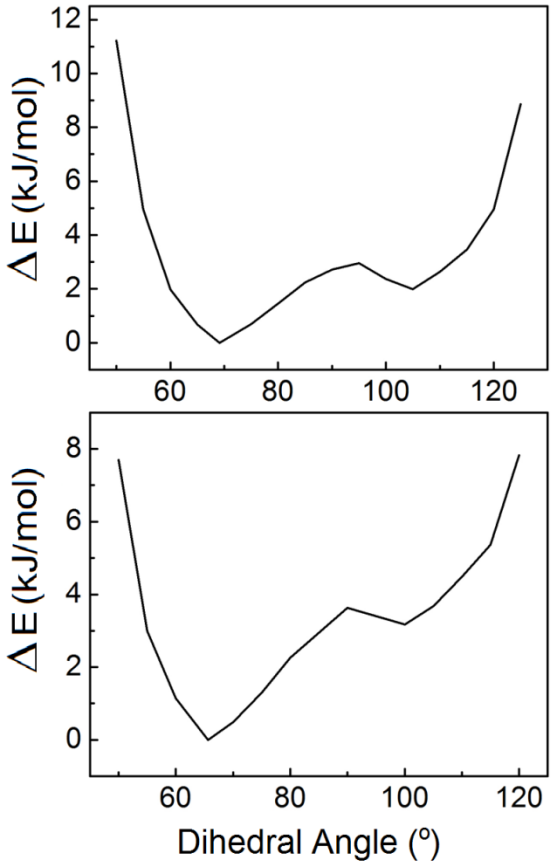

Figure S23. Change in total energy of **1** upon the change in dihedral angle formed by the Mg(II)porphyrin and C_6H_4 (up) and between the free base and C_6H_4 average planes (bottom). The minima are respectively, 71.5 and 67.5°.

6. Photophysical spectra and decays

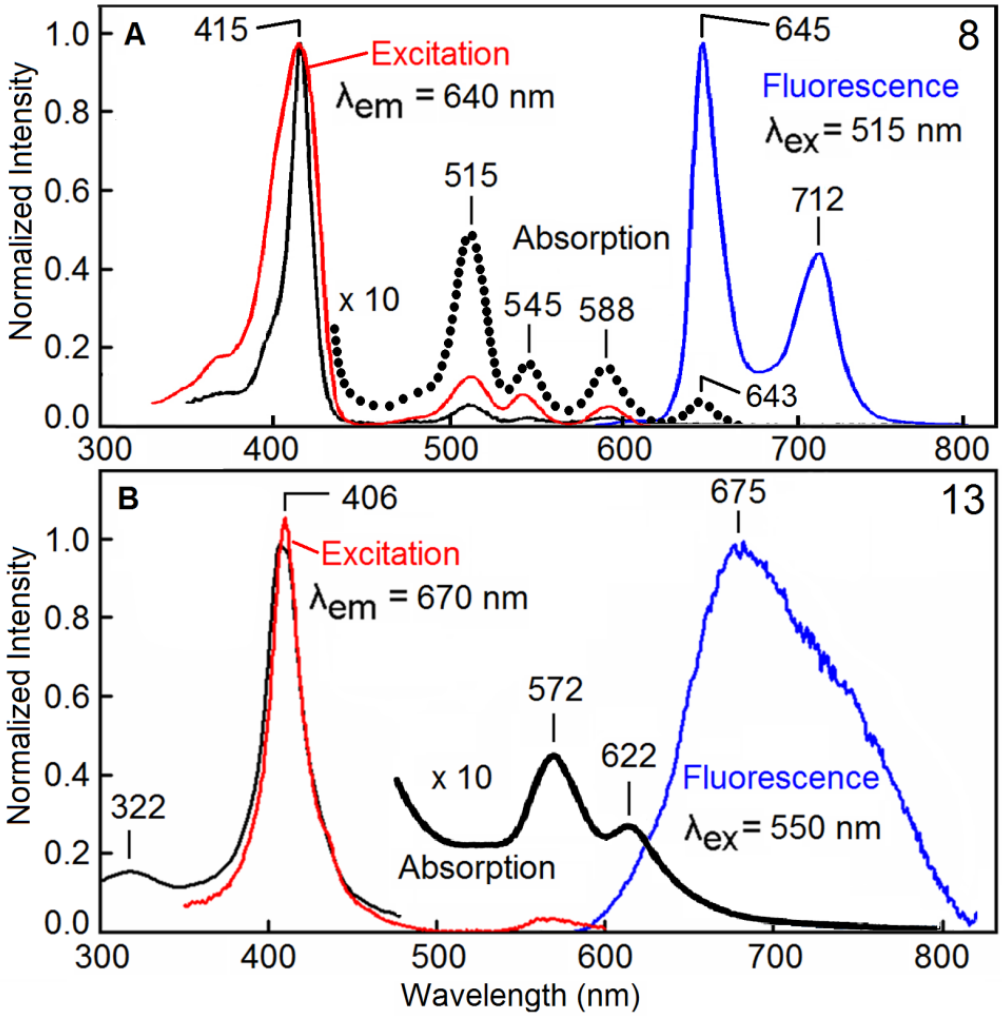

Figure S24 : Absorption (black), fluorescence (blue) and excitation (red) spectra of **8** (up) and **13** (down) in 2MeTHF at 298K.

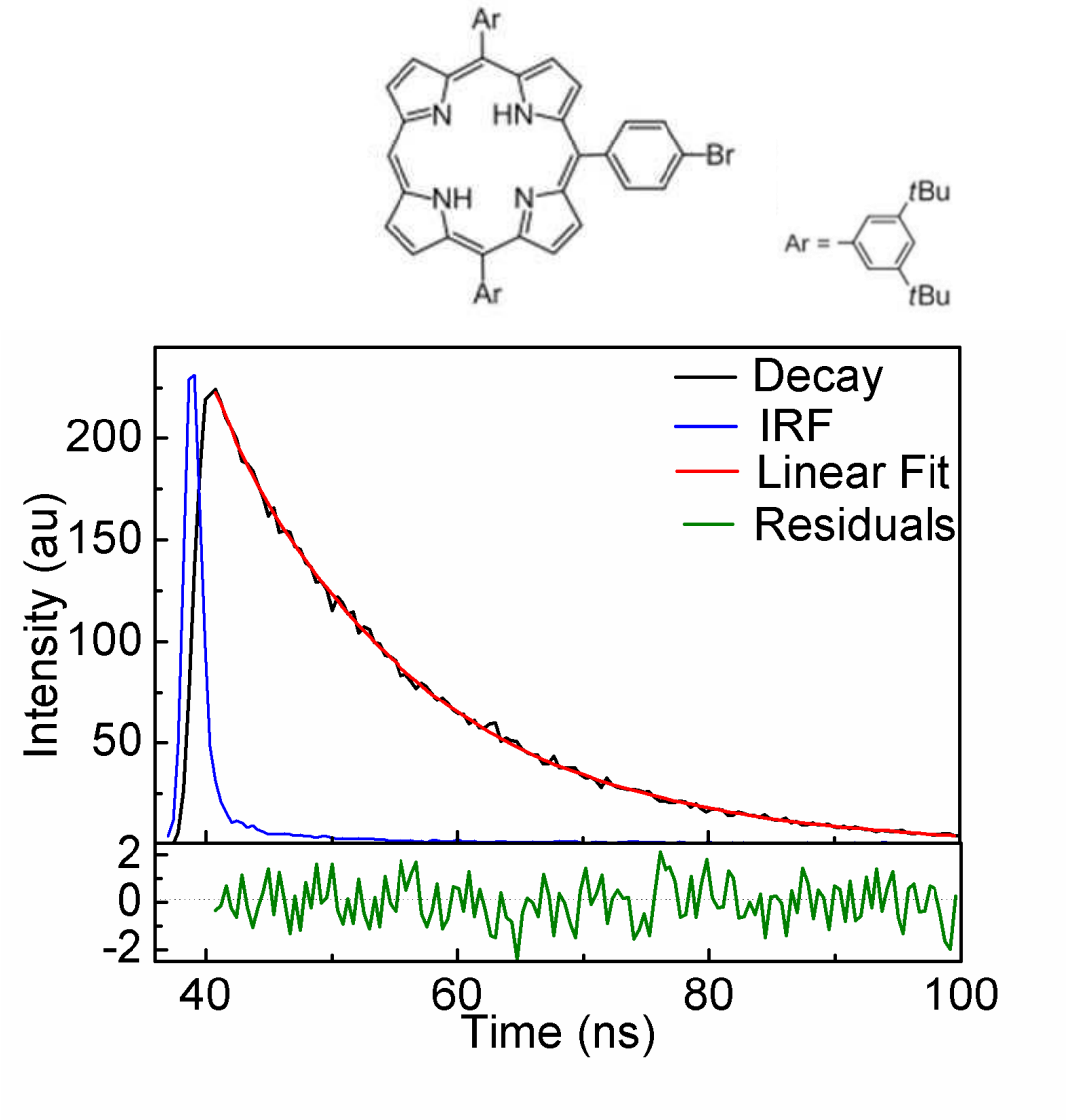

Figure S24 : Fluorescence decay curve for **8** in 2MeTHF at 298K. λ_{exc} = 510 nm, λ_{em} = 645 nm. Pre-exp = 0.537 ± 0.005; lifetime = 13.87 ± 0.11 ns; χ^2 = 0.850.

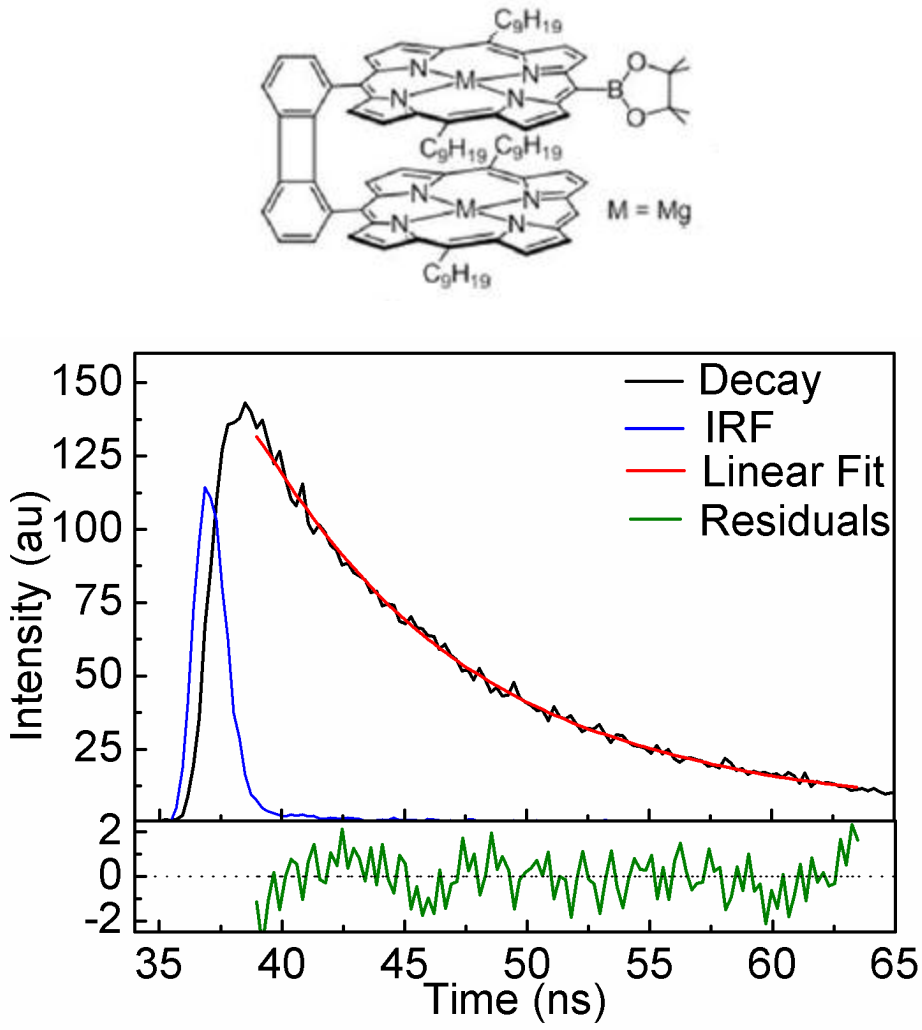

Figure S25 : Log (top) and linear scale (bottom) of the fluorescence decay curve for **13** in 2MeTHF at 298K. λ_{exc} = 595 nm, λ_{em} = 667 nm. Pre-exp = 0.846 ± 0.007; lifetime = 7.58 ± 0.11 ns; χ^2 = 1.049.

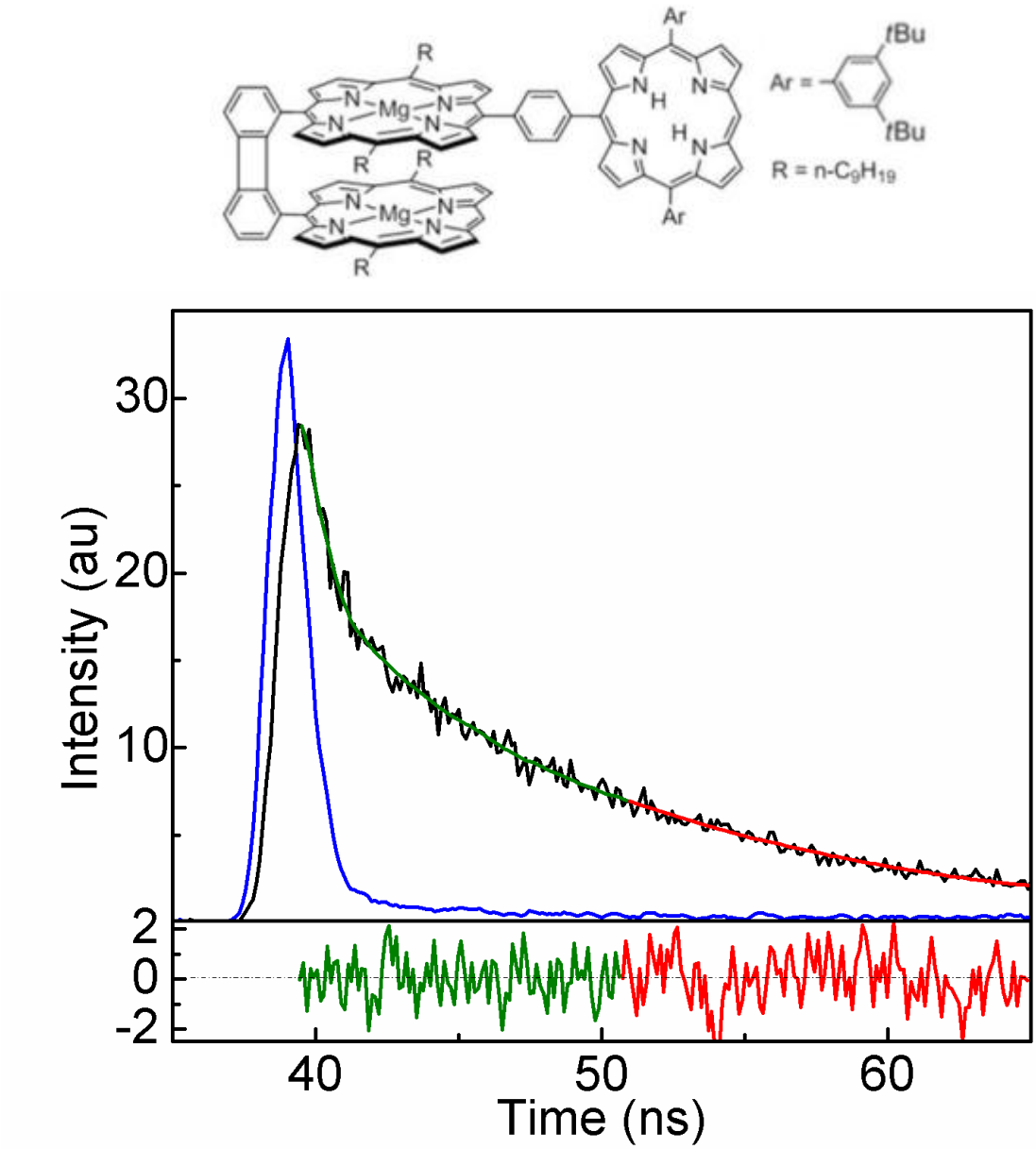

Figure S26. Fluorescence decay curve for **1** in 2MeTHF at 298K. λ_{exc} = 510 nm, λ_{em} = 720 nm. Fit for the first half (in green): Pre-exp. 1 = 2.45 ±0.79, lifetime 1 = 0.21 ± 0.06; Pre-exp. 2 = 0.329 ±0.001, lifetime 2 = 7.11 ± 0.85; χ^2 = 0.865. Fit for the second half (in red): Pre-exp. = 0.335 ± 0.018; lifetime = 11.2 ± 1.20; χ^2 = 1.127. The relative low counts of the decays are due to the sensibility limit of the Strobe detection.

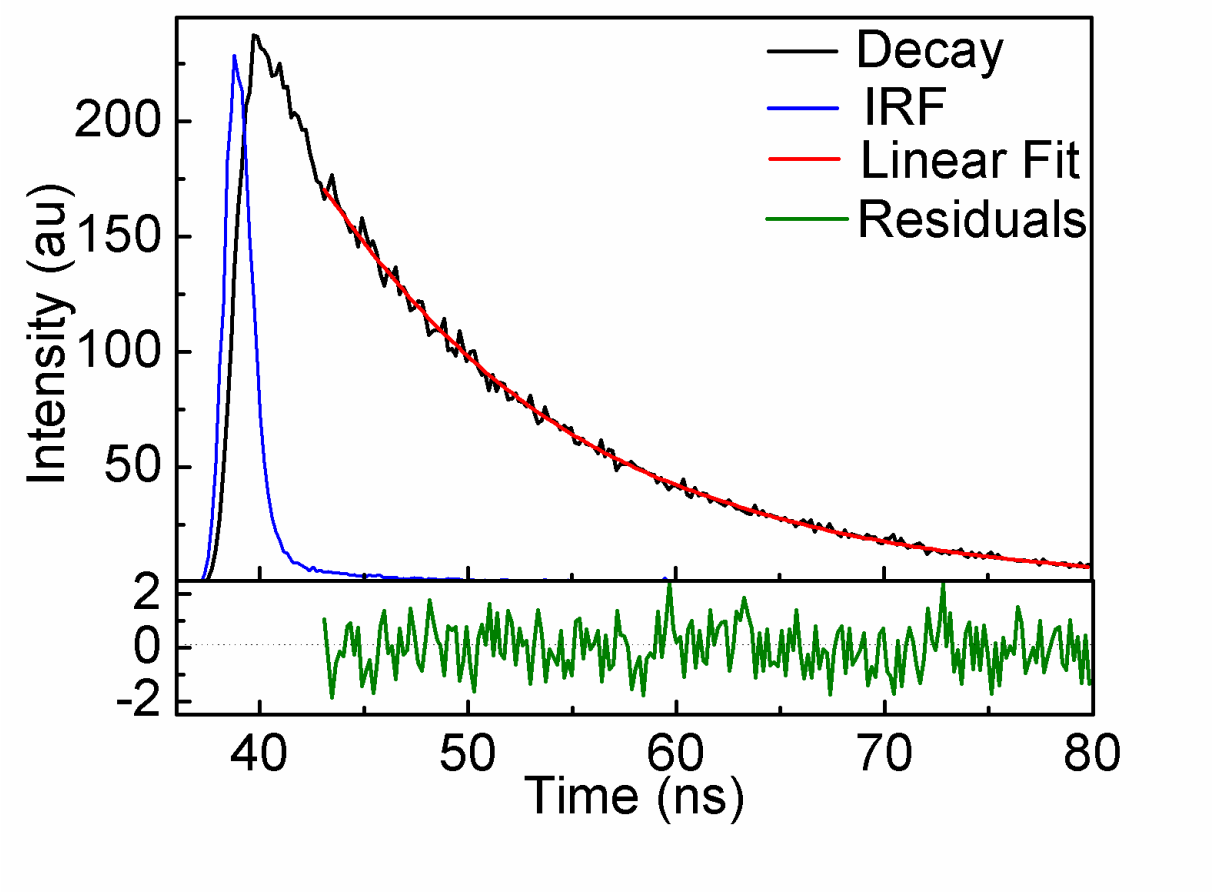

Figure S27. Fluorescence decay curve for **1** in 2MeTHF at 298K. λ_{exc} = 510 nm, λ_{em} = 670 nm. Pre-exp. = 0.601 ± 0.004, lifetime = 10.99 ± 0.08; χ^2 = 0.8043. The slower components of 0.21 and 7.1 ns associated with the bis(porphyrin unit) are not accurately determined in this decay due to their lower relative intensity.

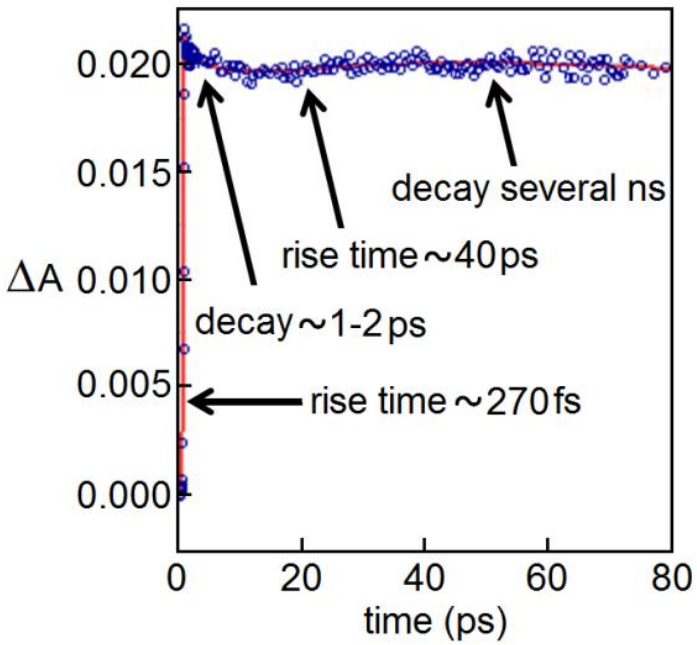

Figure 28. Rise and decay traces for the transient absorption spectra of **1** in 2MeTHF at 298 K monitored at 480 nm. Laser excitation = 400 nm, pulse width = 0.12 ps, laser power = 0.5 mJ/pulse, abs at 400 nm = 0.1. Note that the shape of the traces remains the same for wavelength > 480 nm. Because the time scale cannot exceed more than 3 ns on this apparatus, the long-lived components cannot be accurately analyzed.